Lyapunov-based Controllers of an n-link Prismatic Robot Arm

Ronal P. Chand †,*, Sandeep A. Kumar ‡, Ravinesh Chand † and Robert Tamath‡

***Abstract*—This research provides a generalized stabilizing velocity controllers for planer robot arm with a base rotational joint and $n \in \mathbb{N}$ translation joint for navigation. The end-effector of the planer robot arm has to navigate from an initial to a final configuration space in an environment, which cluttered with obstacles. The velocity controllers are developed from a Lyapunov function, total potentials, designed via Lyapunov-based control scheme (LbCS) falling under the classical approach of artificial potential fields method. The effectiveness of the controllers is validated through computer simulations.**

I. Introduction

High quality and speed needs of our globalized contemporary world's manufacturing systems require a wide range of technical and technological developments. Unfortunately, human efforts to complete activities in hostile circumstances have resulted in numerous threats to the lives of those engaged and errors causing loss of capital. Moreover, humans are bound to work at certain hours, which is incompetent at the rate at which production is required to meet necessities to enjoy a comfortable life. Robots are meant to undertake dull, dirty, and dangerous activities in situations and environments inaccessible or hazardous to humans [1], [2]. They are programmed to accomplish a wide range of speed and precision in various scenarios and environments. Robots are used in multiple works worldwide, including people rescue [3], [4], navigation [5]–[10], ocean cleanup and discovery [11], [12], retail supplementation [13], health care needs [3], [14], [15], and agricultural assistance [16].

Robots consist of several essential components, such as manipulators, control systems, power supply, sensors, and software to execute a task. Aerial and ground vehicles, swimming and flying robots, parallel robotic systems, car-like and tractor-trailers, and mobile manipulators are among mechanical systems is mainly investigated. Robots are being researched for use in a variety of industries, including transportation, agriculture, companionship, medical treatment and surgery, search and rescue, pursuit-evasion, and explorations, to mention a few. Furthermore, certain robots are intended to accomplish specific tasks since each working environment in which robots operate necessitates developing extra capabilities to achieve peak performance. Segway is a well-known two-wheeled, self-balancing personal transporter and can help reduce traffic problems in cities and pollution [17]. For persons who have difficulty walking, robotic wheelchairs can assist them [18]. For space exploration, remotely operated vehicles and remote manipulator systems are developed [19].

One of the essential aspects of a robot is its arm. A robotic arm is a mechanical component that performs functions comparable to a human arm, is a mechanically articulated system made up of links connected by joints, and is usually programmable. The arm can be the sum of the mechanism or part of a larger robot. The joints are mainly of two types: revolute and prismatic. While a prismatic joint provides a linear mechanism by allowing relative translation about an axis, a revolute joint allows relative rotation between two links, allowing for a more complex linear mechanism. The arm has an end-effector that enables it to pick and place objects. The component could be made by revolute joints only or a combination with prismatic to achieve its desired objectives. There are both anchored arms and non-anchored arms. An anchored arm is fixed at a particular place to carry out tasks at the fixed position, whereas an unanchored arm is a component of mobile manipulators.

Many methods are used to solve the path and motion planning problem in robotics. These techniques are eventually classified as heuristics approaches or non- heuristics approaches. Each technique has advantages and disadvantages due to its design strategies and tends to be more appropriate in a situation. Artificial Potential Field (APF) is one of the most commonly used methods of classical approach used to develop robot mechanical systems as the success are shown in [20], [21]. It possesses two potential field forces: repulsive and attractive. When the robot switches from its initial to final configuration, the APF ensures a safe path by enabling the repulsive force towards obstacles and the attraction force towards the target. It does, however, have a limitation due to its local minima. APF have many techniques, one of which is the Lyapunov function. The robotic arm has made essential contributions to a wide variety of current applications. These manipulators are capable of doing repetitive operations at a higher rate of speed, such as pick-up and delivery in hospitals [22]. [23]used the Lyapunov technique to solve the obstacle avoidance problem for a 2-link revolute manipulator in an obstacle-ridden workspace.

This paper aims to develop generalized stabilizing velocity controllers for a planer robot arm consisting of a base rotational joint and $n \in \mathbb{N}$ translation joint in an environment with

† School of Mathematical & Computing Sciences, Fiji National University, Suva, Fiji.

‡ School of Information Technology, Engineering, Mathematics & Physics, The University of the South Pacific, Suva, Fiji.

*Corresponding author email: ronal.chand@fnu.ac.fj

stationary obstacles. Lyapunov-based control scheme (LbCS) will be used to create a total potential, Lyapunov function, from which the nonlinear time invariant controllers for motion and path planning of RP^n robot arm is derived.

The rest of the paper is organized as follows: The Lyapunov-based Control Scheme is briefly described in Section II, and the robot arm system modeling is shown in Section III. Then, in Section IV, velocity controllers are derived using LbCS, and in Section V, simulation results are presented. Finally, in Section VI, concluding remarks are made.

II. Lyapunov-based Control Scheme

LbCS is the construction of artificial potential fields such an attractive field is created towards the target, and a repulsive field is created from each obstacle. As a result, these functions become a component of total potentials, referred to as the Lyapunov function in this context. Using LbCS, the nonlinear stabilizing controllers based on velocity or acceleration could be employed. In [3], [20], [24]–[33], it has been demonstrated that a range of problems is doable. The essential advantage of adopting LbCS is that the continuous controllers can be simply deduced in [1], [20], [31], which is a significant advantage over other approaches. LbCS, on the other hand, has the disadvantage of the possibility of algorithm singularities (local minima) occurring.

III. System Modelling

The planer robot arm consists of a base rotational joint and $n \in \mathbb{N}$ translation joint in the z_1z_2-plane as shown in Fig 1. The first link is a revolute (R) and other links are prismatic (P) with varying length. From now onward, the abbreviation RP^n will be considered as the planer robot arm shown in Fig 1. With the illustration of Fig 1, it is assumed that

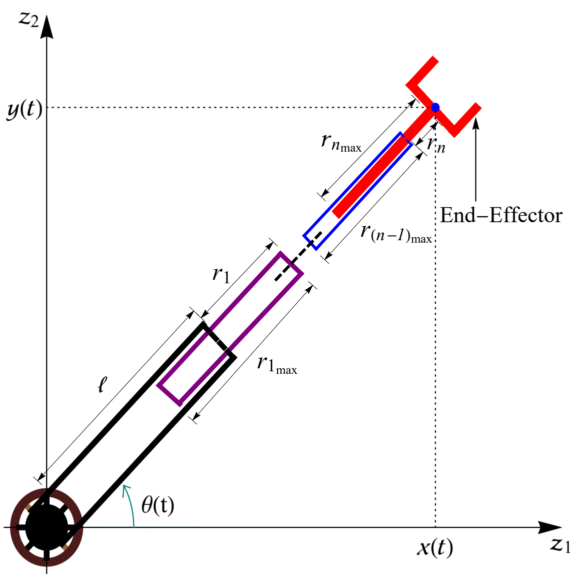

Fig. 1. Representation of a planer RP^n Manipulator.

i. the planer RP^n manipulator is anchored at the origin;
ii. the revolute link has a fixed length l;
iii. the manipulator has an angular position $\theta(t)$ at time t with respect to z_1 axis;
iv. the k^{th} prismatic link has a maximum length $r_{k_{max}}$ where $k = \{1, 2, 3, ..., n\}$ and $r_k(t)$ is the extracted length of the k^{th} prismatic link; and
v. the coordinate of the end-effector is

$$(x(t), y(t)) := (\cos\theta(t)(l + \sum_{k=1}^{n} r_k(t)),$$
$$\sin\theta(t)(l + \sum_{k=1}^{n} r_k(t)).$$

It is thus necessary to design a set of differential equations that accurately depicts the motion of an n-link revolute manipulator arm with a prismatic end-effector. Let $\boldsymbol{x} = (x(t), y(t))$ be the position of the gripper of robot arm at time $t \geq 0$. Additionally, $x(t)$ and $y(t)$ are the x-component and y-component of the end-effector's position, respectively. The angular velocity of the robot arm and the linear velocity of the k^{th} prismatic link for $k = \{1, 2, 3, \ldots, n\}$ are given by $\theta'(t) = \omega(t)$ and $r'_k(t) = \upsilon_k(t)$, respectively. The kinematic model suppressing t of the robot arm is as follows:

$$\left.\begin{aligned} \dot{x} &= \cos\theta \sum_{k=1}^{n} \upsilon_k - \omega y, \\ \dot{y} &= \sin\theta \sum_{k=1}^{n} \upsilon_k + \omega x, \\ \dot{\theta} &= \omega, \\ \dot{r}_k &= \upsilon_k. \end{aligned}\right\} \tag{1}$$

The initial condition at $t_0 \geq 0$ are as $x_0 := x(t_0)$, $y_0 := y(t_0)$, $\theta_0 := \theta(t_0)$, $r_{k_0} := r_k(t_0)$. Suppressing t, the state vector could be written as $\mathbf{x} := (x, y, \theta, r_1, r_2, ..., r_n) \in \mathbb{R}^{n+3}$and $\mathbf{x}_0 := (x_0, y_0, \theta_0, r_{1_0}, r_{2_0}, ..., r_{n_0}) \in \mathbb{R}^{n+3}$. The instantaneous velocity (ω, υ_k) has a state feedback law with the following structure:

$$\omega(t) := -\mu f(\mathbf{x}(t)), \text{ and } \upsilon(t) \quad := -\varphi_k g_k(\mathbf{x}(t)),$$

where $k \in \{1, 2, 3, ..., n\}$. Note that μ, φ_k are some scalars and $f(\mathbf{x}(t))$, and $g_k(\mathbf{x}(t))$ are some function to be constructed later. We can define $\boldsymbol{G}(\mathbf{x}) := (-\mu f(\mathbf{x}), -\varphi_1 g_1(\mathbf{x}), -\varphi_2 g_2(\mathbf{x}), ..., -\varphi_n g(\mathbf{x})) \in \mathbb{R}^{n+1}$,then

$$\dot{\mathbf{x}} = \boldsymbol{G}(\mathbf{x}), \ \mathbf{x}(t_0) = \mathbf{x}_0. \tag{2}$$

Definition 3.1: The ultimate target for the RP^n robot arm manipulator is a disk with the center $\mathbf{x}_\tau = (a, b)$ and radius of r_τ. It is defined as the set:

$$T := \{(z_1, z_2) \in R^2 : (z_1 - a)^2 + (z_2 - b)^2 \leq r_\tau^2\}.$$

Definition 3.2: The equilibrium point for the RP^n robot arm manipulator is described as:

$$\mathbf{x}_e := (a, b, \theta_f, r_{1_f}, r_{2_f}, ..., r_{n_f}) \in \mathbb{R}^{n+3}$$

where θ_f represents the orientation angle of the robotic arm and r_{k_f} is the final extension of the k^{th} prismatic link with $k \in \{1, 2, 3, \dots, n\}$.

IV. Velocity controllers

Consider a workspace of RP^n robotic arm cluttered with $q \in \mathbb{N}$ disk type obstacles. The end-effector of the RP^n robotic arm has to navigate to the target location from its initial state.

A. Lyapunov Function Components

1) Target Attraction: To ensure that the end-effector of the robotic arm converges to its equilibrium position, it is necessary to use a radically unbounded function to the target.

$$H(\boldsymbol{x}) = \frac{1}{2}\left\|\boldsymbol{x} - \boldsymbol{x}_\tau\right\|^2. \tag{3}$$

2) Limitation and Restriction: It should be noted that the $(k+1)^{th}$ prismatic link cannot be fully inserted into the k^{th} link. The restriction on the k^{th} prismatic link is that $r_k(t) \neq 0$ at any time t, that is $r_{k_0} = r_k(0) > 0$ for $k = \{1, 2, 3, ..., n\}$. The limitation is that $r_{k_{max}} - r_k(t) \geq r_0$ at any time t. To avoid these singularities, the following functions are defined:

$$S_k = r_k(t) \text{ and } Q_k = r_{k_{max}} - r_k(t),$$

where $r_{k_{max}}$ is the total length of the k^{th} prismatic link.

3) Stationary Obstacle Avoidance:

Definition 4.1: The i^{th} solid stationary obstacle is a disk with center $\boldsymbol{x}_{O_i} = (o_{x_i}, o_{y_i})$ and radius $r_{O_i} > 0$. It is described as the set

$$O_i = \{(z_1, z_2) \in \mathbb{R}^2 : (z_1 - o_{x_i})^2 + (z_2 - o_{y_i})^2 \leq r_{O_i}^2\}.$$

For the robotic arm to avoid the i^{th} stationary obstacle, for $i \in \{1, 2, 3, \dots, q\}$, a point on the robotic arm that is closest to the obstacle is found, where the minimum distance technique (MDT) is used to minimize the distance function

$$D_i = \left\|(X_i, Y_i) - \boldsymbol{x}_{O_i}\right\|,$$

The robot arm could be described by the line segment respect to time using θ. To avoid obstacles with center (o_{x_i}, o_{y_i}) and radius of $r_{o_i}^2$ it is significant to avoid the line given by the equation

$$X_i = x - \lambda_i \cos\theta \sum_{k=1}^{n} r_k(t),$$
$$Y_i = y - \lambda_i \sin\theta \sum_{k=1}^{n} r_k(t),$$

where

$$\lambda_i = \min\{\max\{0, \Omega\}, 1\}$$

and

$$\Omega = \frac{\cos\theta(x - o_{x_i}) + \sin\theta(y - o_{y_i})}{\sum_{k=1}^{n} r_k(t)}.$$

For the purpose of avoiding the i^{th} stationary solid obstacle where $i \in \{1, 2, 3, \dots, q\}$, we adopt the following obstacle avoidance function

$$W_i = \frac{1}{2}[(X_i - o_{x_i})^2 + (Y_i - o_{y_i})^2 - r_{O_i}^2]. \tag{4}$$

4) A Lyapunov Function: Let $\alpha > 0$,$\gamma_k > 0$,$\Upsilon_k > 0$ and $\beta_i > 0$ be real numbers, and for $k = \{1, 2, 3, ..., n\}$ and $i = \{1, 2, 3, ..., q\}$,the Lyapunov function suppressing t for system (1) becomes

$$L(\mathbf{x}) = H(\boldsymbol{x})\left(\alpha + \sum_{k=1}^{n}\frac{\gamma_k}{Q_k} + \sum_{k=1}^{n}\frac{\Upsilon_k}{S_k} + \sum_{i=1}^{q}\frac{\beta_i}{W_i}\right).$$

5) Velocity Controllers: Alone the trajectory of the system (2),

$$\begin{aligned}\dot{L}(\mathbf{x}) \;=\; & \dot{H}(\boldsymbol{x})\left(\alpha + \sum_{k=1}^{n}\frac{\gamma_k}{Q_k} + \sum_{k=1}^{n}\frac{\Upsilon_k}{S_k} + \sum_{i=1}^{q}\frac{\beta_i}{W_i}\right) \\ & -\dot{H}(\boldsymbol{x})\left(\sum_{k=1}^{n}\frac{\gamma_k}{Q_k^2}\dot{Q}_k + \sum_{k=1}^{n}\frac{\Upsilon_k}{S_k^2}\dot{S}_k\right) \\ & -\sum_{i=1}^{q}\frac{\beta_i \dot{H}(\boldsymbol{x})}{W_i^2}\dot{W}_i\end{aligned}$$

which can be simplified to

$$\dot{L}(\mathbf{x}) = f(\mathbf{x})\omega + \sum_{k=1}^{n} g_k(\mathbf{x})\upsilon_k. \tag{5}$$

Note the $f(\mathbf{x}) = \dfrac{\partial L(\mathbf{x})}{\partial \theta}$ and $g_k(\mathbf{x}) = \dfrac{\partial L(\mathbf{x})}{\partial r_k}$. Let there be constants $\mu, \varphi_k > 0$ for $k = \{1, 2, 3, ..., n\}$, then

$$\omega = -\mu f(\mathbf{x}), \text{ and } \upsilon_k = -\varphi_k g_k(\mathbf{x}) \tag{6}$$

V. Stability Analysis

The $L(\mathbf{x})$ is positive over the domain

$$\begin{aligned}D(L(\mathbf{x})) \;:=\; & \Big\{\mathbf{x} \in \mathbb{R}^{n+3}, Q_k > 0, S_k > 0, \\ & W_i > 0, \forall k = \{1, 2, 3, ..., n\}, \\ & \forall i = \{1, 2, 3, ..., q\}\Big\}\end{aligned}$$

Substituting (6) into (5) gives,

$$\dot{L}(\mathbf{x}) = -\left(\mu f^2(\mathbf{x}) + \sum_{k=1}^{n}\varphi_k g_k^2(\mathbf{x})\right) \leq 0. \tag{7}$$

The system (2) can be seen as having $L(\mathbf{x}_e) = 0$, and $L(\mathbf{x}) > 0, \forall \mathbf{x} \neq \mathbf{x}_e$, and by (7) $\dot{L}(\mathbf{x}) \leq 0$. Thus, it is worth noting that the system (2) is stable.

VI. Simulation Work

The Wolfram Mathematica 12.1 program was used to create the computer simulations in this study. Several Mathematica commands were run in succession in order to get the required results. Using the brute-force approach, it is necessary to determine the values of the convergence, system singularities, and restriction avoidance parameters prior to executing the algorithm. With the RK4 (Runge-Kutta Method) technique, a numerical simulation of the system was performed.

This section will consider two scenarios. The first scenario will be on RP^3 robot arm with one obstacle in its path. The second scenario will be on RP^4 robot arm with two obstacles in its path.

A. RP^3 robot Arm with one Obstacle

In this scenario we choose a robot arm with 3 prismatic links and an anchored revolute joint at $(0, 0)$. The robot arm at $t = 0$ and the trajectory taken can be seen Fig 2. The length of the revolute link is $l_1 = 4$, and the initial length of prismatic links are as $r_1 = 0.7$, $r_2 = 0.6$, $r_3 = 0.5$ with $r_{k_{max}} = 2.5$. The convergence parameters are $\mu = 0.001$, $\varphi_k = 0.0002$, $\alpha = 0.5$, $\beta = 0.01$, $\gamma_k = \Upsilon_k = 0.0004$ where $k = \{1, 2, 3\}$. Note that there is only one obstacle thus $i = 1$.

The Lyapunov function $L > 0$ and decreases in each time interval till the system reaches its equilibrium state at its corresponding target as shown in Fig 3. The Lyapunov function $\dot{L}(\mathbf{x}) < 0$ is also shown in Fig 3. In Fig 4 three different positions of robot arm are shown where $t = 50$, $t = 240$ and $t = 1550$. At $t = 1550$ the robot arm successfully reaches to its target by avoiding a obstacles in its path.

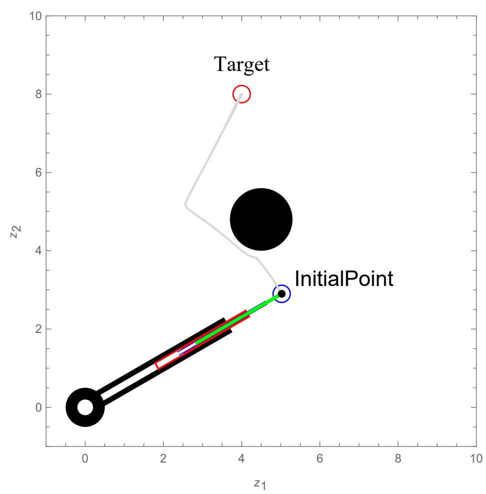

Fig. 2. The positions of robot arm at $t = 0$.

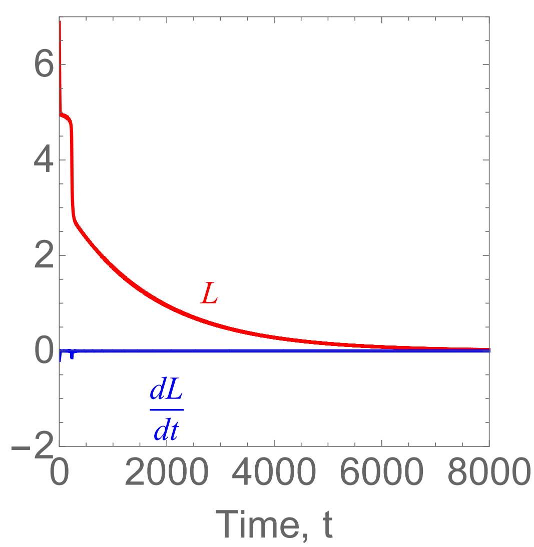

Fig. 3. The evolution of Lyapunov function, and its time derivative.

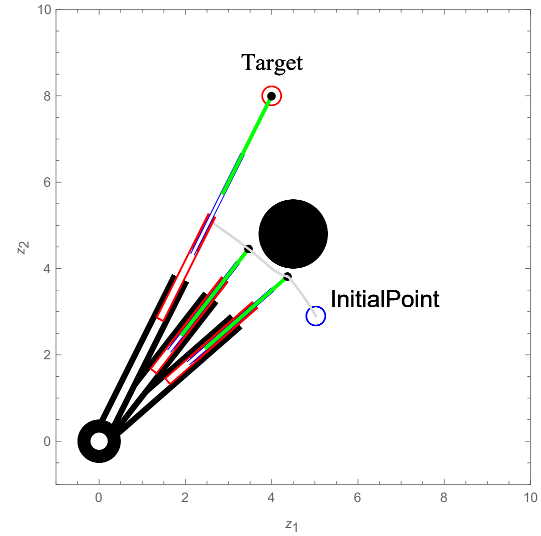

Fig. 4. The position of robot arm $t = 50$, $t = 240$ and $t = 15520$.

B. RP^4 robot Arm with two Obstacles

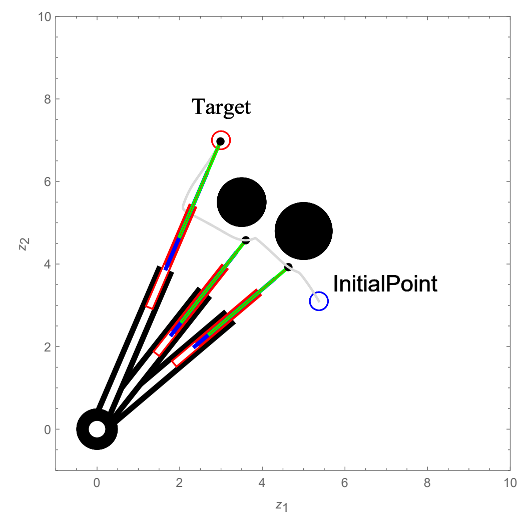

Fig. 5. The position of robot arm $t = 87$, $t = 537$ and $t = 8979$.

In this scenario we choose a robot arm with 3 prismatic links and an anchored revolute joint at $(0, 0)$. The length of the revolute link is $l_1 = 4$, and the initial length of prismatic links are as $r_1 = 0.7$, $r_2 = 0.6$, $r_3 = 0.5$, $r_4 = 0.4$ with $r_{k_{max}} = 2.5$. The convergence parameters are $\mu = 0.001$, $\varphi_k = 0.0002$, $\alpha = 0.5$, $\beta_1 = \beta_2 = 0.01$, $\gamma_k = \Upsilon_k = 0.0004$ where $k = \{1, 2, 3, 4\}$. Note that there two obstacle in this scenario, thus $i = 2$. In Fig 5 three different position of robot arm are shown where $t = 87$, $t = 537$ and $t = 8979$. At $t = 18979$ the robot arm successfully reaches to its target by avoiding obstacles in its path.

VII. Conclusion

This paper presented stabilizing velocity controllers for a generalized planer robot arm consisting of a base rotational joint and $n \in \mathbb{N}$ translation joint. The controllers enable the end-effector to navigate from its initial state to its goal in an environment cluttered with obstacles. Numerical examples validate the controllers designed. This model can be extended whereby the arm has to achieve subgoals in an environment which is cluttered with various types of obstacles.

Acknowledgement

The authors of this article would like to acknowledge Dr. Bibhya Sharma who is an Associate Professor of Mathematics in the School of Information Technology, Engineering, Mathematics and Physics at The University of the South Pacific for his comments which led to the enhancement of the quality and presentation of this research article.

References

[1] B. Sharma, J. Vanualailai, and S. Singh. Motion planning and posture control of multiple n-link doubly nonholonomic manipulators. *Robotica*, 35(1):1–25, 2017.

[2] J. Vanualailai, A. Sharan, and B. Sharma. A swarm model for planar formations of multiple autonomous unmanned aerial vehicles. In *2013 IEEE International Symposium on Intelligent Control (ISIC)*, pages 206–211, 2013.

[3] S. A. Kumar and J. Vanualailai. A Lagrangian UAV swarm formation suitable for monitoring exclusive economic zone and for search and rescue. In *2017 IEEE Conference on Control Technology and Applications (CCTA)*, pages 1874–1879, 2017.

[4] S. A. Kumar, J. Vanualailai, and A. Prasad. Distributed velocity controllers of the individuals of emerging swarm clusters. In *2020 IEEE Asia-Pacific Conference on Computer Science and Data Engineering (CSDE)*, pages 1–6, 2020.

[5] A. Prasad, B. Sharma, and J. Vanualailai. A new stabilizing solution for motion planning and control of multiple robots. *Robotica*, 34(5):1071 – 1089, 2016.

[6] B. Sharma, J. Vanualailai, and A. Prasad. Formation control of a swarm of mobile manipulators. *The Rocky Mountain Journal of Mathematics*, pages 909–940, 2011.

[7] A. Prasad, B. Sharma, and S. A. Kumar. Strategic creation and placement of landmarks for robot navigation in a partially-known environment. In *2020 IEEE Asia-Pacific Conference on Computer Science and Data Engineering (CSDE)*, pages 1–6, 2020.

[8] A. Prasad, B. Sharma, J. Vanualailai, and S. A. Kumar. A geometric approach to target convergence and obstacle avoidance of a nonstandard tractor-trailer robot. *International Journal of Robust and Nonlinear Control*, 30(13):4924–4943, 2020.

[9] A. Prasad, B. Sharma, J. Vanualailai, and S. A. Kumar. Stabilizing controllers for landmark navigation of planar robots in an obstacle-ridden workspace. *Journal of Advanced Transportation*, 2020, 2020.

[10] K. Raghuwaiya, J. Vanualailai, and B. Sharma. Formation splitting and merging. In Ying Tan, Yuhui Shi, and Li Li, editors, *Advances in Swarm Intelligence*, pages 461–469, Cham, 2016. Springer International Publishing.

[11] Juan Rojas. Plastic waste is exponentially filling our oceans, but where are the robots?, 2018.

[12] Oussama K., Xiyang Y., Gerald B., Brian S., Boyeon K., Shameek G., Hannah S., Shiquan W., Mark C., Aaron E., Phillip M., Mitchell B., Christian R. V., Khaled N. S., Michel L., and Vincent C. Ocean one: A robotic avatar for oceanic discovery. *IEEE Robotics Automation Magazine*, 23(4):20–29, 2016.

[13] Dhruv G., Anne L. R., and Jens N. The future of retailing. *Journal of Retailing*, 93(1):1–6, 2017. The Future of Retailing.

[14] Z. Lu, A. Chauhan, F. Silva, and L. S. Lopes. A brief survey of commercial robotic arms for research on manipulation. In *2012 IEEE Symposium on Robotics and Applications (ISRA)*, pages 986–991, 2012.

[15] A. Gilmour, A. D. MacLean, P. J. Rowe, M. S. Banger, I. Donnelly, B. G. Jones, and M. J.G. Blyth. Robotic-arm–assisted vs conventional unicompartmental knee arthroplasty. the 2-year clinical outcomes of a randomized controlled trial. *The Journal of arthroplasty*, 33(7):S109–S115, 2018.

[16] L. C. Santos, F. N. Santos, E. J. Solteiro P., A. Valente, P. Costa, and S. Magalhães. Path planning for ground robots in agriculture: a short review. In *2020 IEEE International Conference on Autonomous Robot Systems and Competitions (ICARSC)*, pages 61–66, 2020.

[17] A. Maddahi, A. H. Shamekhi, and A. Ghaffari. A Lyapunov controller for self-balancing two-wheeled vehicles. *Robotica*, 33:225–239, 2015.

[18] B. Borges, A. Chandra, R. Kalantri, S. Gupta, G. Dsilva, and S. Rajguru. Android controlled wheelchair. In *2018 First International Conference on Secure Cyber Computing and Communication (ICSCCC)*, pages 1–7, 2018.

[19] G. Hirzinger. Space robotics. *IFAC Proceedings Volumes*, 27(14):695–714, 1994. Fourth IFAC Symposium on Robot Control, Capri, Italy, September 19-21, 1994.

[20] S. A. Kumar, J. Vanualailai, B. Sharma, and A. Prasad. Velocity controllers for a swarm of unmanned aerial vehicles. *Journal of Industrial Information Integration*, 22:100198, 2021.

[21] A. Prasad, B. Sharma, J. Vanualailai, and S. A. Kumar. Motion control of an articulated mobile manipulator in 3d using the Lyapunov-based control scheme. *International Journal of Control*, pages 1–15, 2021.

[22] B. Kumar, L. Sharma, and S. Wu. Job allocation schemes for mobile service robots in hospitals. In *2018 IEEE International Conference on Bioinformatics and Biomedicine (BIBM)*, pages 1323–1326. IEEE, 2018.

[23] A. Prasad, B. Sharma, and J. Vanualailai. Motion control of a 2-link revolute manipulator in an obstacle-ridden workspace. *International Journal of Mathematical, Computational, Physical, Electrical and Computer Engineering*, 6(12):1751–1756, 2012.

[24] S. A. Kumar, J. Vanualailai, and A. Prasad. Assistive technology: autonomous wheelchair in obstacle-ridden environment. *PeerJ Computer Science*, 7:e725:1–23, 2021.

[25] S. A. Kumar, B. Sharma, J. Vanualailai, and A. Prasad. Stable switched controllers for a swarm of UGVs for hierarchal landmark navigation. *Swarm and Evolutionary Computation*, 65:100926, 2021.

[26] S. A. Kumar, J. Vanualailai, and B. Sharma. Lyapunov functions for a planar swarm model with application to nonholonomic planar vehicles. In *2015 IEEE Conference on Control Applications (CCA)*, pages 1919–1924, 2015.

[27] S. A. Kumar, J. Vanualailai, and B. Sharma. Lyapunov-based control for a swarm of planar nonholonomic vehicles. *Mathematics in Computer Science*, 9(4):461–475, October 2015.

[28] B. Sharma, J. Vanualailai, and S. Singh. Lyapunov-based nonlinear controllers for obstacle avoidance with a planar n-link doubly nonholonomic manipulator. *Robotics and Autonomous Systems*, 60(12):1484–1497, December 2012.

[29] K. Raghuwaiya, B. Sharma, and J. Vanualailai. Cooperative control of multi-robot systems with a low-degree formation. In H. Sulaiman, M. Othman, M. Othman, Y. Rahim, and N. Pee, editors, *Advanced Computer and Communication Engineering Technology. Lecture Notes in Electrical Engineering.*, volume 362, pages 233–249. Springer, 2016.

[30] S. A. Kumar, J. Vanualailai, B. Sharma, A. Chaudary, and V. Kapadia. Emergent formations of a Lagrangian swarm of unmanned ground vehicles. In *Proceedings of the 2016 14th International Conference on Control, Automation, Robotics and Vision, ICARCV 2016*, Phuket, Thailand, November 2016. IEEE.

[31] B. N. Sharma, J. Raj, and J. Vanualailai. Navigation of carlike robots in an extended dynamic environment with swarm avoidance. *International Journal of Robust and Nonlinear Control*, 28(2):678–698, 2018.

[32] V. Chand, A. Prasad, K. Chaudhary, B. Sharma, and S. Chand. A face-off-classical and heuristic-based path planning approaches. In *2020 IEEE Asia-Pacific Conference on Computer Science and Data Engineering (CSDE)*, pages 1–6, 2020.

[33] A. Devi, J. Vanualailai, S. A. Kumar, and B. Sharma. A cohesive and well-spaced swarm with application to unmanned aerial vehicles. In *Proceedings of the 2017 International Conference on Unmanned Aircraft Systems*, pages 698–705, Miami, FL, USA, June 2017.